# Endotoxin producers overgrowing in human gut microbiota as the causative agents for nonalcoholic fatty liver disease

Na Fei, Aurelia Bruneau, Xiaojun Zhang, Ruirui Wang, Jinxing Wang, Sylvie Rabot, Philippe Gerard, Liping Zhao

AMERICAN SOCIETY FOR MICROBIOLOGY | mBio®

RESEARCH ARTICLE
Host-Microbe Biology

# Endotoxin Producers Overgrowing in Human Gut Microbiota as the Causative Agents for Nonalcoholic Fatty Liver Disease

**Na Fei,[a] Aurélia Bruneau,[a] Xiaojun Zhang,[b] Ruirui Wang,[b] Jinxing Wang,[b] Sylvie Rabot,[a] Philippe Gérard,[a] Liping Zhao[b,c]**

[a]Université Paris-Saclay, INRAE, AgroParisTech, Micalis Institute, Jouy-en-Josas, France
[b]State Key Laboratory of Microbial Metabolism, School of Life Sciences and Biotechnology, Shanghai Jiao Tong University, Shanghai, People's Republic of China
[c]Ministry of Education Key Laboratory for Systems Biomedicine, Shanghai Centre for Systems Biomedicine, Shanghai Jiao Tong University, Shanghai, People's Republic of China

**ABSTRACT** Gut microbiota-derived endotoxin has been linked to human nonalcoholic fatty liver disease (NAFLD), but the specific causative agents and their molecular mechanisms remain elusive. In this study, we investigated whether bacterial strains of endotoxin-producing pathogenic species overgrowing in obese human gut can work as causative agents for NAFLD. We further assessed the role of lipopolysaccharide (LPS)-Toll-like receptor 4 (TLR4) cross talk in this pathogenicity. Nonvirulent strains of Gram-negative pathobionts were isolated from obese human gut and monoassociated with C57BL/6J germfree (GF) mice fed a high-fat diet (HFD). Deletion of *waaG* in the bacterial endotoxin synthetic pathway and knockout of TLR4 in GF mice were used to further study the underlying mechanism for a causal relationship between these strains and the development of NAFLD. Three endotoxin-producing strains, *Enterobacter cloacae* B29, *Escherichia coli* PY102, and *Klebsiella pneumoniae* A7, overgrowing in the gut of morbidly obese volunteers with severe fatty liver, induced NAFLD when monoassociated with GF mice on HFD, while HFD alone did not induce the disease in GF mice. The commensal *Bacteroides thetaiotaomicron* (ATCC 29148), whose endotoxin activity was markedly lower than that of *Enterobacteriaceae* strains, did not induce NAFLD in GF mice. B29 lost its proinflammatory properties and NAFLD-inducing capacity upon deletion of the *waaG* gene. Moreover, *E. cloacae* B29 did not induce NAFLD in TLR4-deficient GF mice. These nonvirulent endotoxin-producing strains in pathobiont species overgrowing in human gut may work as causative agents, with LPS-TLR4 cross talk as the most upstream and essential molecular event for NAFLD.

**IMPORTANCE** Recent studies have reported a link between gut microbiota and nonalcoholic fatty liver disease (NAFLD), showing that germfree (GF) mice do not develop metabolic syndromes, including NAFLD. However, the specific bacterial species causing NAFLD, as well as their molecular cross talk with the host for driving liver disease, remain elusive. Here, we found that nonvirulent endotoxin-producing strains of pathogenic species overgrowing in obese human gut can act as causative agents for induction of NAFLD and related metabolic disorders. The cross talk between endotoxin from these specific producers and the host's TLR4 receptor is the most upstream and essential molecular event for inducing all phenotypes in NAFLD and related metabolic disorders. These nonvirulent endotoxin-producing strains of gut pathogenic species overgrowing in human gut may collectively become a predictive biomarker or serve as a novel therapeutic target for NAFLD and related metabolic disorders.

**KEYWORDS** gut inflammation, intestinal microbiology, fatty liver, nonalcoholic steatohepatitis, gut inflammation

**Citation** Fei N, Bruneau A, Zhang X, Wang R, Wang J, Rabot S, Gérard P, Zhao L. 2020. Endotoxin producers overgrowing in human gut microbiota as the causative agents for nonalcoholic fatty liver disease. mBio 11: e03263-19. https://doi.org/10.1128/mBio.03263-19.

**Editor** Edward G. Ruby, University of Hawaii at Manoa



Address correspondence to Philippe Gérard, philippe.gerard@inrae.fr, or Liping Zhao, lpzhao@sjtu.edu.cn.

This article is a direct contribution from Liping Zhao, a Fellow of the American Academy of Microbiology, who arranged for and secured reviews by Jun Yu, Institute of Digestive Diseases, Prince of Wales Hospital, The Chinese University of Hong Kong, and Fabienne Foufelle, INSERM UMRS 1138, Sorbonne Université, Sorbonne Paris Cité, Université Paris Descartes, Université Paris Diderot, Centre de Recherche des Cordeliers, Paris, France.

**Received** 21 December 2019
**Accepted** 2 January 2020
**Published** 4 February 2020

Nonalcoholic fatty liver disease (NAFLD) has become the most common cause of chronic liver disease strongly associated with a high risk of obesity and type 2 diabetes (1). During the past decade, evidence for cross talk between the gut microbiome, the liver, the immune system, and metabolism has emerged, suggesting that the resident microbiota has emerged as an important player in the development of NAFLD (2).

Recently, causal evidence for gut microbiota involvement in the pathogenesis of NAFLD has been shown in mice and in humans by transplanting the whole gut microbiota to germfree (GF) mice (3, 4). High-fat diet (HFD)-fed GF mice exhibit lower levels of lipids in the liver than conventionally housed mice (3, 4), indicating that HFD is not sufficient for disease development. Gut microbiota from mice that developed fasting hyperglycemia and insulinemia, but not from healthy mice, led to the development of NAFLD in recipient GF mice (5). Fecal transplantation from human donors with hepatic steatosis triggered a rapid development of hepatic steatosis in mice (6). Gut microbiota from obese humans, but not from the same donor after weight loss, induced the onset of hepatic steatosis through modulation of lipid metabolism transcriptional profiles in GF mice (7). HFD-fed GF mice inoculated with microbiota of nonalcoholic steatohepatitis (NASH) patients, rather than healthy donors, showed an exacerbated NAFLD phenotype, as manifested by increased liver steatosis and inflammation (8). Collectively, these pieces of evidence indicate a causal role of the gut microbiota in the development of NAFLD (9).

NAFLD has been associated with increased levels of specific Gram-negative bacterial species, including *Proteobacteria*, *Enterobacteria*, *Escherichia* (10, 11), and *Bacteroides* (11, 12). A higher representation of *Gammaproteobacteria* and *Epsilonproteobacteria* was also seen in children with NAFLD than in healthy lean and obese children (13). These studies indicated an association between Gram-negative bacteria and progression of NAFLD. However, strains from the same species may have different functions due to the still high genetic diversity (14). Moreover, these studies failed to causally identify microorganisms that differentiate individuals with the disease and the control population.

Activation of innate immunity is associated with the development of NAFLD (15). Gut-derived toxins, such as endotoxins, are suggested to have causative roles in liver inflammation, as well as the onset and progression of chronic liver diseases (16). Serum LPS levels are increased in patients with hepatic steatosis caused by total parenteral nutrition or intestinal bypass (17, 18). In mice on standard laboratory chow, continuous subcutaneous infusion of low-dose LPS results in hepatic steatosis, hepatic insulin resistance, and hepatic weight gain (19). In addition, an intraperitoneal injection of LPS exacerbates liver injury in mice fed a methionine-choline-deficient diet (20). The LPS-binding protein (LBP)-CD14 complex activates Toll-like receptor 4 (TLR4), triggering an essential inflammatory cascade in the progression of NAFLD (21, 22). These data indicate that the liver is the main target of LPS, and LPS-TLR4 is a key pathway. However, the role of specific bacteria and their bioactive molecules and their contribution to the inflammation-driven process in NAFLD remain to be definitively identified and demonstrated as the cause.

We previously showed that one nonvirulent, endotoxin-producing strain, B29, from the sepsis-inducing species *Enterobacter cloacae*, overgrowing in the gut of an obese human, can induce obesity when monocolonized in GF mice on HFD (23). The primary aim of the present study was to establish a definitive cause-effect link between the endotoxin producers enriched in obese subjects and NAFLD development. We also want to further elucidate the molecular cross talk between these bacteria and their host in the initiation and progression of this disease.

## RESULTS

**Human case study. (i) Volunteer 1.** Volunteer 1 was a 26-year-old morbidly obese man (weight, 174.8 kg; height, 172.5 cm; body mass index [BMI], 58.78 kg/m$^2$; Taiyuan city, Shanxi Province, China) with coexisting metabolic syndrome (23). Besides obesity,

this volunteer also had severe fatty liver, as observed by ultrasonography, with concomitant markedly increased levels of serum concentrations of aspartate aminotransferase (122 U liter$^{-1}$), alanine aminotransferase (97 U liter$^{-1}$), and gamma-glutamyl transferase (168 U liter$^{-1}$) (23).

This volunteer was given a diet composed of whole grains, traditional Chinese medicine, and prebiotics (WTP diet) for 23 weeks. He lost 30.1 kg after 9 weeks and 51.4 kg after 23 weeks on the diet, with continued amelioration of hyperinsulinemia, hyperglycemia, hypertension, and liver function until most metabolic parameters improved to normal ranges. *Enterobacter* made up 35% of the gut bacteria in volunteer 1 at the beginning, and after 9 weeks on the WTP diet, the *Enterobacter* population in the volunteer's gut reduced to 1.8% and became undetectable by the end of the 23-week trial (23). Details were presented in our previous study. *Enterobacter cloacae* B29 was isolated from the baseline fecal sample of this volunteer as the most abundant pathobiont. *Klebsiella pneumoniae* A7 was isolated from the same volunteer's gut as the second most abundant pathobiont (23).

**(ii) Volunteer 2.** Volunteer 2 was a 3-year-old morbidly obese girl (Chinese; initial body weight, 46 kg; Shanxi Province, China) with coexisting metabolic syndrome. *Escherichia coli* was detected as 40% of her gut microbiota, as shown using sequencing of the V3 region of the 16S rRNA gene (data not published). She lost 16 kg after 20 weeks with alleviated fatty liver phenotype on the WTP diet, and the *E. coli* population was reduced to nondetectable soon after she was on the diet. *Escherichia coli* PY102 was isolated from the feces of volunteer 2 via a sequence-guided isolation scheme (23 and data not published).

***E. cloacae* B29 acts as a causative agent for NAFLD induction in GF mice under HFD feeding.** To test whether nonvirulent endotoxin-producing strains of gut pathogenic species overgrowing in obese human gut can act as causative agents for NAFLD induction, we inoculated $10^9$ to $10^{10}$ cells of *E. cloacae* B29 into C57BL/6J GF mice fed either a normal chow diet (NCD) or HFD. *E. cloacae* B29 achieved a population level of between $10^9$ and $10^{10}$ cells/g of feces (see Fig. S1 in the supplemental material). At the end of the trial, NCD-fed mice colonized with wild-type *E. cloacae* B29 showed no significant difference in the features of NAFLD (Fig. 1A to C) and gained a similar amount of body weight (Fig. 1D to F and Fig. S2) compared to the NCD-fed control mice. On the contrary, HFD-fed mice colonized by *E. cloacae* B29 (termed HFD+B29), but not the HFD-fed GF control mice, were characterized by significantly enhanced hepatic steatosis and NAFLD activity scores (Fig. 1A to C), among other obesity-related phenotypes. These mice also displayed significantly higher body weight than the HFD-fed GF control mice (Fig. 1D and Fig. S2) despite possessing the smallest cecum of all the mice (GF mice normally possess a significantly bigger cecum than the conventional mice) (Fig. S2) (24). The HFD+B29 mice also exhibited a significant increase in fat mass (epididymal, mesenteric, subcutaneous inguinal, and retroperitoneal fat pads) (Fig. 1E and F) and blood lipid concentration (Fig. S2) compared to levels of all other groups. Moreover, the increases in serum leptin concentration and epididymal fat pad *Leptin* gene expression level were observed in HFD+B29 mice (Fig. S2). The obese HFD+B29 mice also exhibited statistically significant elevations in blood glucose and insulin levels (both fasted and 30 min postchallenge) and a marked decrease in glucose tolerance relative to all other groups (Fig. 1G and H), consistent with features of insulin resistance. We also found significantly increased expression of fatty acid synthase (*Fas*) and peroxisome proliferator-activated receptor-gamma (*Pparγ*) in the liver and fat pad and decreased expression of fasting-induced adipose factor (*Angptl4*) in the liver and ileum of HFD+B29 mice (Fig. S2), indicating a disrupted lipometabolism favoring synthesis or storage but not removal of fat. Inflammation plays a critical role in NAFLD development (25). Elevated serum levels of LBP and proinflammatory cytokine serum amyloid A protein (SAA-3) and increased expression of the *Tlr4* gene in the liver (Fig. 2A and B) were detected in the HFD+B29 mice but not the HFD-fed GF control mice (Fig. 2A and B). In agreement with these results, gene expression analysis revealed

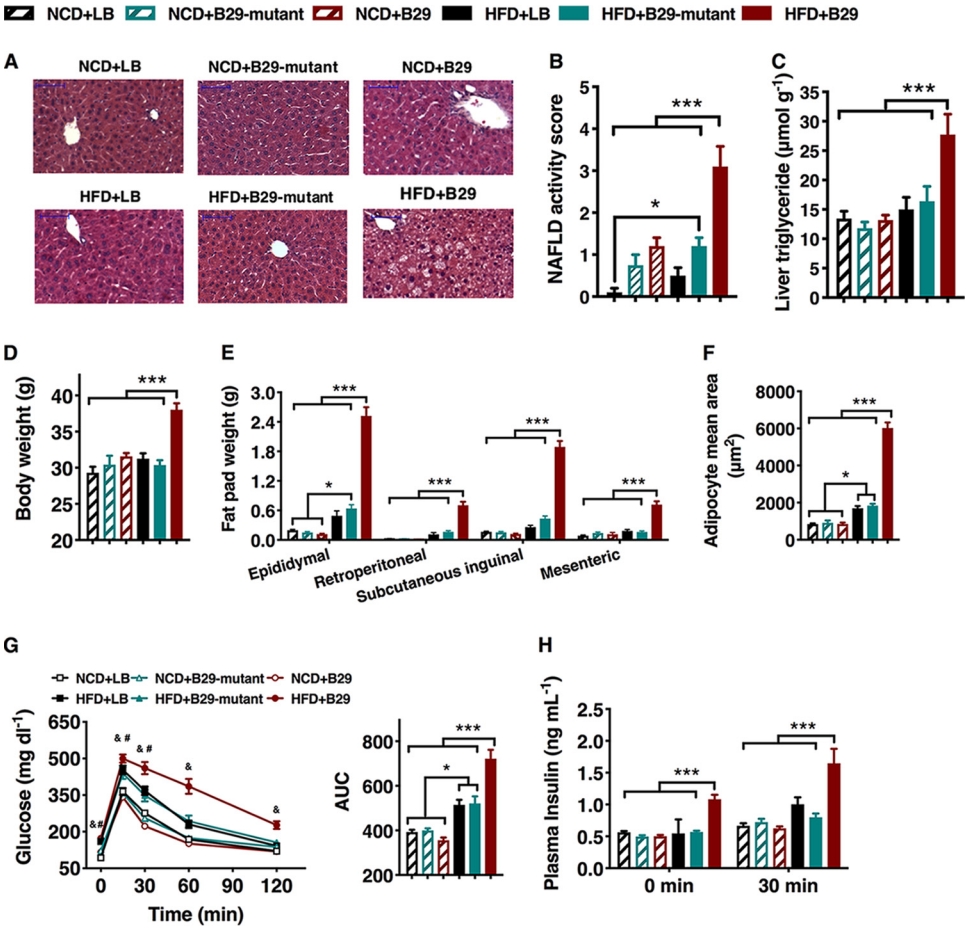


**FIG 1** *E. cloacae* B29-dependent induction of NAFLD in GF mice under HFD feeding requires endotoxin expression. Germfree (GF) mice were fed either normal chow diet (NCD) or high-fat diet (HFD) and inoculated with either Luria-Bertani (LB), wild-type *E. cloacae* B29, or the endotoxin-lacking *waaG* mutant strain (data were collected at the end of 15 weeks after inoculation). (A) Liver histology (hematoxylin and eosin stain). Scale bar, 50 $\mu$m. (B) NAFLD activity score. (C) Liver triglyceride. (D) Body weight. (E) Mass of epididymal, mesenteric, subcutaneous inguinal, and retroperitoneal fat pads. (F) Adipocyte mean area. (G) Oral glucose tolerance test (OGTT) and the area under the curve (AUC) for the plasma glucose concentration ($P < 0.05$; &, HFD+B29 versus other groups; #, HFD+LB and HFD+B29-mutant versus NCD groups). (H) Plasma insulin concentration before (fasting) and 30 min after oral glucose load. Data shown are means ± SEM ($n = 5$ to 10). *, $P < 0.05$; **, $P < 0.01$; ***, $P < 0.001$.

significantly elevated levels of mRNA corresponding to the proinflammatory cytokines tumor necrosis factor alpha (*Tnfα*), interleukin-1$\beta$ (*Il1β*), interleukin-6 (*Il6*), monocyte chemoattractant protein-1 (*Mcp1-Ccl2*), and inhibitor of $\kappa$B kinase epsilon (*Ikkε*) in the liver and adipose tissue and c-type lectin-regenerating islet-derived protein 3-$\gamma$ (*Reg3γ*) in the gut of HFD+B29 mice compared to those of the other groups (Fig. 2D to F). In summary, all features of NAFLD and metabolic abnormalities were observed only in HFD+B29 mice. This indicates that *E. cloacae* B29 works as a causative agent for NAFLD while HFD works as the necessary environmental factor, which itself does not induce the disease.

***E. cloacae* B29 induction of systemic and local inflammation in HFD-fed NAFLD GF mice is dependent upon endotoxin expression.** To demonstrate that the production of proinflammatory LPS endotoxin from the gut pathogenic species is essential for inducing NAFLD and subsequent metabolic complications in mice, we deleted the *waaG* gene of *E. cloacae* B29 (26). *waaG* is involved in the synthesis of LPS and encodes a protein that joins the outer core and O-antigen parts of the LPS molecule by catalyzing the transfer of a glucose moiety from the donor nucleotide sugar UDP-α-D-glucose to the L-glycero-D-manno-heptose II of the inner core of LPS (26, 27). The LPS

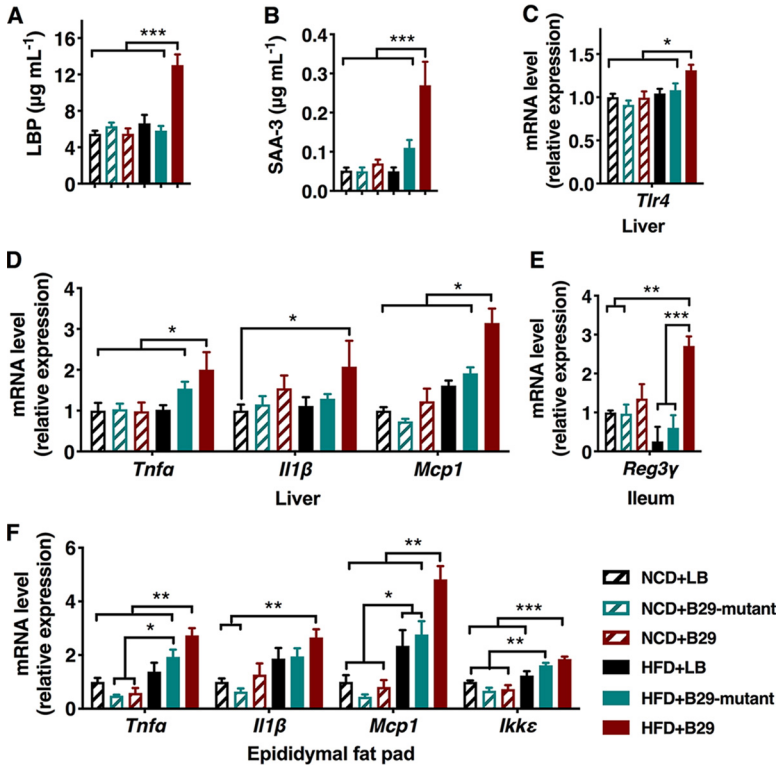


**FIG 2** *E. cloacae* B29 induction of systemic and local inflammation in HFD-fed NAFLD GF mice is dependent upon endotoxin expression. GF mice were fed either normal chow diet (NCD) or high-fat diet (HFD) and inoculated with either Luria-Bertani broth (LB), wild-type *E. cloacae* B29, or the endotoxin-lacking *waaG* mutant strain (data were collected at the end of 15 weeks after inoculation). (A) ELISA of serum LPS-binding protein (LBP). (B) ELISA of serum amyloid A (SAA-3). (C) RT-qPCR analysis of expression of the *Tlr4* gene in the liver. (D to F) RT-qPCR analysis of expression of the *Tnfα*, *Il1β*, *Mcp1*, *Ikkε*, and *Reg3γ* genes in the liver (D), ileum (E), and epididymal fat pad (F). All mRNA quantification data were normalized against the housekeeping gene. Gene expression levels were expressed as values relative to those of the control group (NCD+LB). *Tlr4*, toll-like receptor 4 gene; *Tnfα*, tumor necrosis factor-α gene; *Il1β*, interleukin-1β gene; *Mcp1*, monocyte chemoattractant protein-1 gene; *Ikkε*, I kappa B kinase epsilon gene; *Reg3γ*, c-type lectin regenerating islet-derived protein 3-γ. Data shown are means ± SEM ($n = 5$ to 10). *, $P < 0.05$; **, $P < 0.01$; ***, $P < 0.001$.

endotoxin activity of the *E. cloacae* B29Δ*waaG* mutant was reduced approximately 600-fold from that of B29 (Fig. S3). Thus, the B29Δ*waaG* mutant essentially lost its proinflammatory capacity.

We then compared the NAFLD-inducing effect of the B29Δ*waaG* mutant to that of its wild-type parent in C57BL/6J GF mice fed on HFD. The B29Δ*waaG* strain also achieved a population level of between $10^9$ and $10^{10}$ cells/g of feces in the gut of gnotobiotic mice (Fig. S1). Intriguingly, at the end of the trial, all features of NAFLD and metabolic abnormalities observed in HFD+B29 mice, including degenerated hepatocytes, increased NAFLD activity score, body weight, fat pad mass, and blood lipid, glucose, and insulin levels, were not observed in mice upon colonization with the *waaG* mutant strain (HFD+mutant) (Fig. 1 and Fig. S2).

We next asked whether deletion of *waaG* gene in *E. cloacae* B29 indeed failed to induce proinflammatory responses in mice. As expected, the elevated serum levels of LBP and proinflammatory cytokine SAA-3 and increased expression of the *Tlr4* gene in the liver of HFD+B29 mice (Fig. 2D) were not detected in the HFD+mutant mice (Fig. 2A and B). In agreement with these results, significantly elevated levels of mRNA corresponding to the proinflammatory cytokines *Tnfα*, *Il1β*, *Il6*, *Mcp1-Ccl2*, and *Ikkε* in the liver and adipose tissue and *Reg3γ* in the gut of HFD+B29 mice were completely absent in HFD+mutant littermates (Fig. 2E to G). Taking these findings together, the B29Δ*waaG* mutant does not induce systemic inflammation or the development of

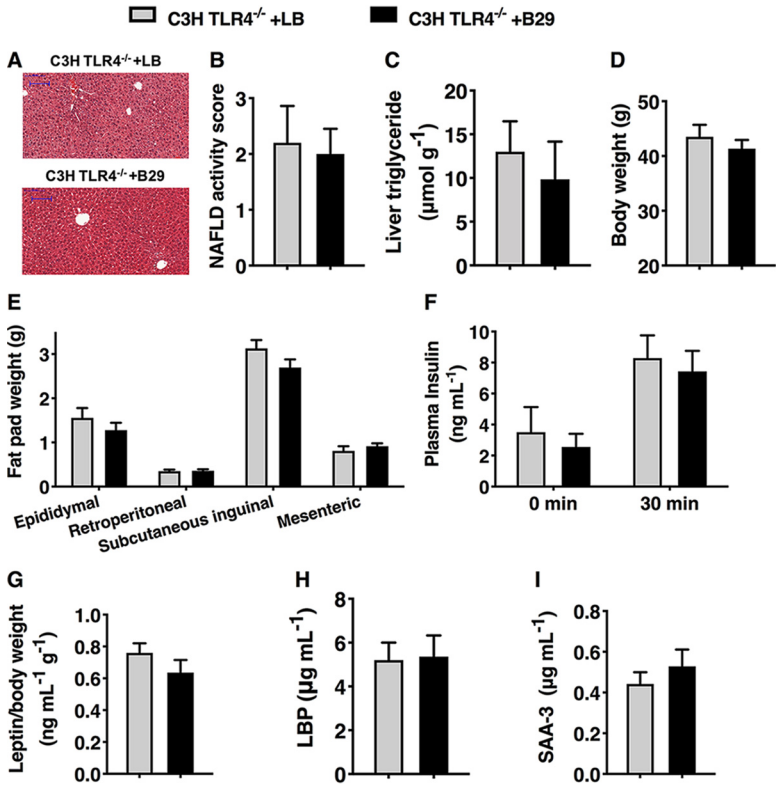


**FIG 3** Absence of TLR4 in mice prevented NAFLD induced by the LPS-producing gut opportunistic pathobiont *Enterobacter cloacae* B29 (data were collected at the end of 15 weeks after inoculation). (A) Liver histology (hematoxylin and eosin stain) of TLR4 mutant (TLR4$^{-/-}$) mice with or without B29 at the end of the trial. Scale bar, 100 $\mu$m. (B) NAFLD activity score. (C) Body weight. (D) Mass of epididymal, mesenteric, subcutaneous inguinal, and retroperitoneal fat pads of TLR4$^{-/-}$mice with or without B29. (E) Plasma insulin concentration before (fasting) and 30 min after oral glucose load in TLR4$^{-/-}$ mice with or without B29. (F) ELISA of serum leptin in TLR4$^{-/-}$ mice with or without B29 (after adjustment for body weight). (G) ELISA of serum LBP in TLR4$^{-/-}$ mice with or without B29. (H) ELISA of serum amyloid A (SAA-3) in TLR4$^{-/-}$ mice with or without B29. Data shown are means ± SEM ($n = 5$ to 9). *, $P < 0.05$; **, $P < 0.01$; ***, $P < 0.001$.

NAFLD in HFD-fed GF mice. This indicates that the proinflammatory capacity of its LPS endotoxin is essential to the NAFLD-inducing property of *E. cloacae* B29.

**Absence of TLR4 in mice prevented NAFLD induced by the LPS-producing gut opportunistic pathobiont *Enterobacter cloacae* B29.** We investigated whether the endotoxin-producing pathobiont *E. cloacae* B29 induces NAFLD in C3H/HeN GF mice with or without TLR4 deficiency to decipher if B29 acts through the LPS-TLR4 signaling pathway and whether its capacity to induce NAFLD is a common phenomenon independent of the genetics of the mouse lines. We analyzed the NAFLD-inducing property of *E. cloacae* B29 with HFD-fed C3H/HeN GF mice with or without TLR4 deficiency. *E. cloacae* B29 achieved a population level of between $10^9$ and $10^{10}$ cells/g of feces, with no significant differences between the gnotobiotic mice with different genetic backgrounds (Fig. S4). HFD-fed wild-type C3H/HeN mice colonized with B29 showed markedly degenerated hepatocytes, a significant increase in NAFLD activity score, obesity, and an insulin-resistant phenotype, unlike the corresponding HFD-fed GF control mice, after 15 weeks of HFD treatment (Fig. S5 and S6). Wild-type C3H/HeN mice colonized with B29 showed significant increases in serum endotoxin load or local and systemic inflammatory levels compared to those of the corresponding GF controls (Fig. S4 and S5). GF TLR4$^{-/-}$ C3H/HeN mice colonized by B29, however, did not develop any NAFLD or other metabolic disease features not seen in noncolonized controls (Fig. 3A to G and Fig. S7). Importantly, *E. cloacae* B29 also failed to induce an endotoxin response or increased downstream inflammatory cytokine production in the GF

TLR4$^{-/-}$ mice compared to that of the corresponding GF control (Fig. 3H and I and Fig. S4). These results indicate that *E. cloacae* B29 is also able to induce NAFLD in C3H/HeN mice and that its NAFLD-inducing capacity requires an intact TLR4 receptor from the host side. TLR4 has been known to be involved in the development of NAFLD (28) and metabolic syndrome (29–32). This study demonstrates that the cross talk between endotoxin from specific producers overgrowing in the obese human gut and the host's TLR4 receptor is the most upstream and essential process for inducing NAFLD. The NAFLD phenotype induced by *E. cloacae* B29 is a common phenomenon independent of the genetics of the mouse lines.

**Gram-negative bacteria producing LPS with different endotoxin activity levels showed different capacities to induce NAFLD in HFD-fed GF mice.** We next hypothesized that this ability to induce inflammation and NAFLD is a more general property of nonvirulent proinflammatory, LPS-producing strains of gut pathogenic species. To test this, we examined the NAFLD-inducing capacity of two other Gram-negative bacteria isolated from the gut of obese volunteers (see Materials and Methods for a detailed description): *Klebsiella pneumoniae* A7 (23) and *Escherichia coli* PY102. *K. pneumoniae* A7 was isolated from the same volunteer's gut as the second most abundant pathobiont (23). *Escherichia coli* was detected as 40% of another obese volunteer's gut microbiota, as shown using sequencing of the V3 region of the 16S rRNA gene (data not published). She lost 16 kg after 20 weeks with alleviated fatty liver phenotype on the WTP diet, and the *E. coli* population was reduced to nondetectable levels soon after she was on the diet. *E. coli* PY102 was isolated from the feces of this volunteer via a sequence-guided isolation scheme (23 and data not published). *K. pneumoniae* A7 and *E. coli* PY102 showed strong endotoxin activity, as determined by the *Limulus* amebocyte lysate (LAL) test (Fig. S8) (33). HFD-fed GF C57BL/6J mice inoculated with *K. pneumoniae* A7 (HFD+*Kleb*) or *E. coli* PY102 (HFD+*E.coli*), reaching a similar bacterial population in the feces (Fig. S8), showed markedly degenerated hepatocytes, significant increase in NAFLD activity score, and associated metabolic syndrome features after 15 weeks of HFD treatment, in contrast to HFD-fed uninfected control mice (Fig. 4A to H and Fig. S9). In addition, HFD+*Kleb* and HFD+*E.coli* mice also displayed a low-grade proinflammatory state, as revealed by markedly increased serum levels of LBP and SAA-3 and high expression levels of certain inflammatory markers, such as *Tnfα* and *Mcp-1*, in the liver, fat pad, and ileum, in contrast to the GF controls (Fig. S8). Taken together, these data suggest that nonvirulent strains of the gut pathogenic species that produce LPS with high endotoxin activity can induce NAFLD and associated metabolic disorders when monocolonized in GF mice fed on HFD.

We next investigated whether a Gram-negative bacterium with nonproinflammatory LPS could also induce NAFLD in GF mice. Previous studies showed that LPS endotoxin activity of *Bacteroides* spp. was 1,000-fold lower than that of species in the *Enterobacteriaceae* family and failed to induce immune activation (34, 35). In light of this evidence, we introduced the commensal bacterium *Bacteroides thetaiotaomicron* type strain (ATCC 29148) to HFD-fed GF C57BL/6J mice (HFD+*B.theta*). The LAL test showed that LPS endotoxin activity from *B. thetaiotaomicron* was nearly 500-fold lower than that from *K. pneumoniae* A7, *E. coli* PY102, and *E. cloacae* B29 (Fig. S8) (36). HFD mice colonized by *B. thetaiotaomicron* exhibited slightly degenerated hepatocytes and significantly increased NAFLD activity scores compared with those of HFD GF mice but markedly lower than those of mice monocolonized with either strain *K. pneumoniae* A7 or *E. coli* PY102 (Fig. 4A and B). Furthermore, mice in group HFD+*B.theta* showed no obesity and an insulin-resistant phenotype (Fig. 4D to H and Fig. S9) (37). HFD+*B.theta* mice showed no significant difference in serum endotoxin load or local and systemic inflammatory levels from levels of the GF control, even though *B. thetaiotaomicron* reached a significantly higher population level in the gut of gnotobiotic mice than either of the other two proinflammatory bacterial strains (Fig. S8). These results further indicate that high endotoxin activity is essential for the NAFLD-inducing function of Gram-negative pathobionts.

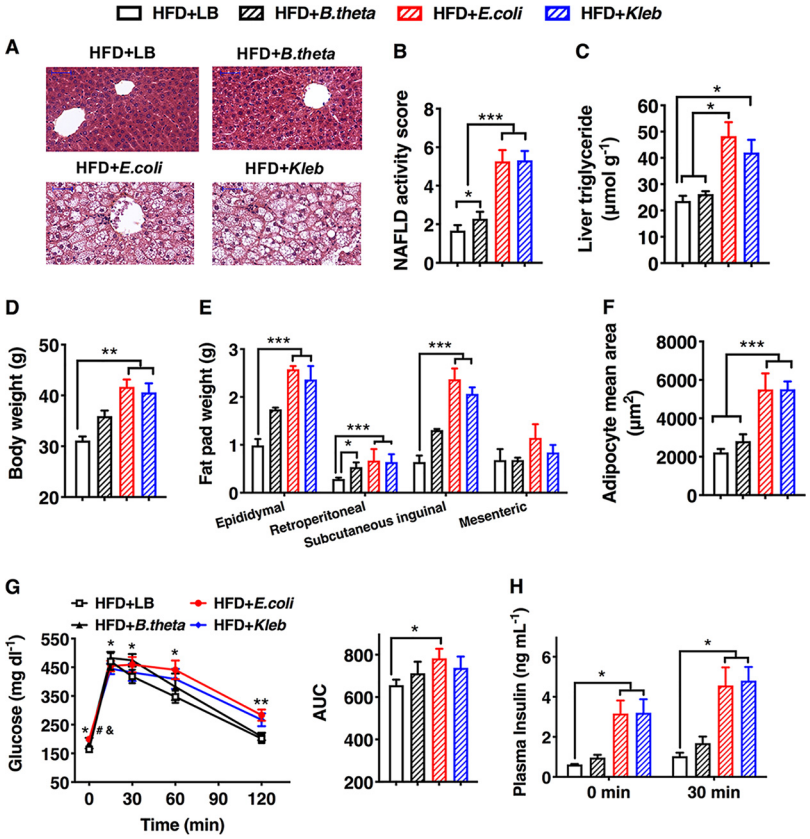


**FIG 4** Gram-negative bacteria producing LPS with different endotoxin activity levels showed different capacities to induce NAFLD in HFD-fed GF mice (data were collected at the end of 15 weeks after inoculation). (A) Liver histology (hematoxylin and eosin stain). Scale bar, 50 $\mu$m. (B) NAFLD activity score. (C) Liver triglyceride. (D) Body weight. (E) Mass of epididymal, mesenteric, subcutaneous inguinal, and retroperitoneal fat pads. (F) Adipocyte mean area. (G) Oral glucose tolerance test (OGTT) and the area under the curve (AUC) for the plasma glucose concentration ($P < 0.05$; #, HFD+LB versus HFD+B.*theta*; &, HFD+LB versus HFD+*Kleb*; *, HFD+LB versus HFD+*E.coli*). (H) Plasma insulin concentration before (fasting) and 30 min after oral glucose load. Data shown are means ± SEM ($n = 7$ to 16). *, $P < 0.05$; **, $P < 0.01$; ***, $P < 0.001$.

The increasing incidence of NAFLD is widely thought to result from nutrient excess due to increased food consumption. We next investigated whether changes in food intake contribute to the NAFLD-inducing effect of gut Gram-negative pathobionts in GF mice. Notably, neither food intake nor gene expression patterns associated with the appetite-regulating peptides (ghrelin, peptide YY, and glucagon-like peptide-1) exhibited differences between mice with and without NAFLD phenotypes on HFD in all the animal trials (Fig. S2L to N and S9L and M). Therefore, the NAFLD-inducing effect of these LPS-producing gut pathobionts is independent of intake of HFD.

## DISCUSSION

During the last 2 decades, major advances have been made in understanding NAFLD's association with gut microbial dysbiosis, providing novel opportunities as well as challenges in both the pathogenesis and treatment options of NAFLD (2). However, the questions of whether specific microbial strains or their consortium can causally trigger NAFLD and become possible therapeutic targets of NAFLD have not been mechanistically addressed. This is of particular interest and importance, since the whole gut microbiota cannot be the targets controlling liver disease (14). Using a monoassociated gnotobiotic model, our previous data support a crucial role for one endotoxin-producing strain, *Enterobacter cloacae* B29, in driving aggressive obesity (23). In the present study, by expanding the previously used approach, we identified that nonvirulent endotoxin-producing strains of pathobiont species overgrowing in the human gut

can work as causative agents with LPS-TLR4 cross talk as the most upstream and essential molecular event for NAFLD and related metabolic disorders.

Until the present study, there has been limited opportunity to explore the putative link between the overgrowing of specific bugs, hepatic fat accumulation, and the development of NAFLD (38). Gram-negative bacteria have been shown to be associated with the progression of NAFLD in cohort studies (10, 11). In the present study, only Gram-negative bacteria belonging to the family *Enterobacteriaceae* with proinflammatory endotoxin (39), like *Enterobacter cloacae* B29, *Klebsiella pneumoniae* A7, and *Escherichia coli* PY102, could induce NAFLD and related metabolic diseases. Conversely, the strains belonging to the family *Bacteroidaceae* that do not have proinflammatory endotoxin, like the *Bacteroides thetaiotaomicron* type strain, exhibited only slightly degenerated hepatocytes compared to those of HFD GF mice. Findings on the effect of *Bacteroides* on the development of metabolic diseases were conflicting in the literature (37). Coinoculation of GF mice with *Bacteroides thetaiotaomicron* and *Methanobrevibacter smithii* has been shown to increase the epididymal fat pad but not the total body weight (37). However, *Bacteroides thetaiotaomicron* was also shown to be markedly decreased in obese individuals and alleviated diet-induced body weight gain and adiposity in mice (40). In this study, we have identified specific noninfectious, endotoxin-producing bacteria as causative agents for the development of NAFLD in humans by following the logic of Koch's postulates (41, 42). First, these bacteria were selected as candidate pathogenic gut bacteria for inducing human NAFLD and related metabolic diseases, because they overgrew as dominant populations before dietary intervention and reduced to almost nondetectable levels soon after the intervention, with the fatty liver phenotype being significantly alleviated (41, 42). For example, in our previous studies, *Enterobacter*, a genus of opportunistic, endotoxin-producing pathogens (39), made up 35% of the total gut bacteria in a morbidly obese volunteer, and this level was reduced to nondetectable after 23 weeks on a diet composed of whole grains, traditional Chinese medicinal foods, and prebiotics (WTP diet), which led to a 51.4-kg weight loss along with the significantly alleviated fatty liver phenotype (23). Similarly, *E. coli* was detected as 40% of the gut microbiota in an obese 3-year-old girl. She lost 16 kg after 20 weeks with alleviated fatty liver phenotype on the WTP diet, and the *E. coli* population was reduced to nondetectable soon after starting the diet. These LPS-producing strains were predominant members of the gut microbiota when their hosts were obese and had fatty liver phenotypes (23). Second, pure cultures of these candidate bacteria were isolated from the human donor samples; in our study, *Enterobacter cloacae* B29 was isolated from the baseline fecal sample of the adult volunteer as the most abundant pathobiont (23). *Klebsiella pneumoniae* A7 was isolated from the same volunteer's gut as the second most abundant pathobiont (23). *Escherichia coli* PY102 was isolated from the baseline sample of a 3-year-old girl. Third, monocolonization of pure culture of these candidate bacteria in GF mice on HFD reproduced NAFLD and other related phenotypes in metabolic syndromes. In the present study, all three Gram-negative bacteria, *Enterobacter cloacae* B29, *Klebsiella pneumoniae* A7, and *Escherichia coli* PY102, could induce NAFLD and related metabolic diseases in GF mice under HFD feeding. Finally, genetic mutations from both the candidate bacteria and host showed that LPS-TLR4 cross talk is required for the initiation and progression of all NAFLD-related phenotypes. Our study provides definitive evidence that specific endotoxin-producing gut bacteria work as causative agents (pathogens) for NAFLD development in humans.

Understanding the mechanisms by which the specific gut microbes influence the progression of NAFLD may allow us to establish gut microbiota-targeted precision medicine in the treatment of NAFLD. At the molecular level, LPS is recognized by the specific pattern recognition receptor TLR4 (43, 44) and its coreceptors, LBP and CD14 (21, 22), which triggers a downstream inflammatory cascade (21, 45). TLR4-deficient mice display decreased liver injury, inflammation, and lipid accumulation compared with wild-type mice in NAFLD models induced by high fructose or NCD diet (28, 46), which confirms the role of TLR4 in inducing inflammation in NAFLD. In accordance with

previous reports, our study shows that the blocking of the LPS-TLR4 interaction between gut pathobionts and host cells can prevent the initiation and development of NAFLD and all other obesity-related phenotypes otherwise inducible on HFD. This indicates that the LPS-TLR4 pathway works as the most upstream molecular event in the specific endotoxin-producing gut bacteria-NAFLD cross talk, consistent with previous research (17, 18). Chronic systemic inflammation driven by these abnormally prevalent pathobiont populations then drives the development of NAFLD and obesity in human hosts (19). Although LPS endotoxin production is essential for these pathobionts to induce NAFLD, as shown in our study, it may not be sufficient. In the complex gut ecosystem, these pathobionts still need to outcompete other bacteria and evade host immune reactions so they can establish a sufficiently higher population level than usual for a long enough time for their proinflammatory properties to come into effect (14, 47).

Our study has some limitations. Except for LPS, other gut microbe-derived components or metabolites, such as peptidoglycans (48), trimethylamine (49), secondary bile acids (50), short-chain fatty acids (51), branched-chain amino acids (52), and ethanol (53), have also been proven to contribute to the regulation of hepatic fat accumulation and the pathogenesis of NAFLD. There have also been many reports of increased intestinal permeability with NAFLD (53–55), which might be an important contributor to disease progression, even though these results were not confirmed in all studies (55). In addition to the LPS-TLR4 pathway, other molecular pathways are involved in the development of NAFLD, and their modulation by specific gut bacteria remains to be established. Adipose tissue also has significant effects on the development of NAFLD (56). For example, the excessive fat deposition in the liver could be initiated by increased fatty acid delivery from adipose tissue (57); hypertrophic and hypoxic adipocytes develop an inflammatory phenotype, secreting inflammatory cytokines into circulation, which induces hepatocyte death and modulates hepatic immune function (58). In our current study, HFD+B29/*Kleb*/*E.coli* gnotobiotic mice had the greatest increase in triglyceride content, suggesting that these mice had the greatest increase in hepatic steatosis; however, the plasma triglyceride concentrations were not modified. Our current study provides *in vivo* evidence to show the causal relationship between the special gut microbes and the development of NAFLD and other related metabolic diseases. However, the molecular mechanisms on the host side underlying the LPS-producing bacteria inducing these metabolic derangements still need further deep investigation. Apolipoprotein B (ApoB) is important in the export of triglycerides from the liver and prevents fatty liver conditions (59). More studies are required to define further the gut microbes that may have a particularly important role in determining the lipid-transporting capability of the ApoB molecule or mitochondrial $\beta$ oxidation in the liver. Distinct microbiome signatures may be associated with different stages of liver diseases, and specific pathobionts may serve as noninvasive microbiota-based predictive or diagnostic biomarkers after their causative role in disease progression has been demonstrated.

In summary, it is imperative to identify NAFLD-related microbes at the strain level. Drawing any clear conclusions on the role of specific bacteria or their consortium in the onset and development of NAFLD has to happen before novel therapy can be developed. Actually, identification of specific gut bacteria mechanistically causing or driving NAFLD is currently in its infancy. Importantly, our data point to a direct pathogenetic role of endotoxin-producing gut bacteria and their molecular cross talk with the host. To the best of our knowledge, this is the first evidence *in vivo* that mechanically shows the association between specific gut taxa and NAFLD. While their implications remain to be refined, the present findings open new avenues for managing NAFLD and related metabolic diseases worldwide.

## MATERIALS AND METHODS

**Animal experimental design.** Germfree (GF) male C57BL/6J mice (provided by Anaxem, the GF animal facility of the Micalis Institute, INRA, Jouy-en-Josas, France), C3H/HeN wild-type mice (provided by

Anaxem), and C3H/HeN TLR4$^{-/-}$ mice (kind gift from the Animal Resources Center, the University of Chicago) were bred under the GF rodent breeding conditions at Anaxem. All mice were maintained on a 12 h-12 h lighted-dark cycle and first supplied with a 45-kGy irradiated sterile pelleted normal chow diet (NCD; energy content of 13.5% fat, 25.2% protein, and 61.3% carbohydrate; standard maintenance diet R03-40; SAFE, France) or high-fat diet (HFD; energy content of 60% fat, 20% protein, and 20% carbohydrate; D12492; Research Diets, Inc., New Brunswick, NJ) and autoclaved tap water *ad libitum*. GF C57BL/6J mice (6 to 8 weeks old) were divided into 4 groups randomly. *E. cloacae* B29 and B29Δ*waaG* strains, *Bacteroides thetaiotaomicron*, *Klebsiella pneumoniae*, or *Escherichia coli* monocolonized mice were obtained by a single intragastric gavage with $10^9$ to $10^{10}$ cells of B29 and B29Δ*waaG* strains, the *B. thetaiotaomicron* type strain (ATCC 29148), *K. pneumoniae* A7, or *E. coli* PY102 per mouse in 0.1 sterile medium fed separately on NCD or HFD. The GF control group was treated with 0.1 ml sterile LB medium per mouse. Each mouse group was raised in a separate isolator and fed on HFD for 15 weeks.

For all animal experiments, body weight and food intake were monitored weekly with an electronic weight indicator (Dini Argeo, Italy). Mice were sacrificed by cervical dislocation, and tissues were collected. Sections of epididymal adipose tissue and the main lobe of liver were fixed in 4% paraformaldehyde–phosphate-buffered saline (PBS) for 48 h and then washed and stored in 70% ethanol. All other sections of the tissues were stored in either liquid nitrogen or RNAlater (Ambion) immediately after exsanguination and stored at −80°C until processing. Details are presented in the supplemental material.

**Bacterial strains.** *Enterobacter cloacae* B29, *K. pneumoniae* A7, and *E. coli* PY102 were grown in LB broth or on LB agar plates at 37°C. The *B. thetaiotaomicron* type strain (ATCC 29148) was cultured in *Bacteroides* bile esculin (BBE) broth at 37°C under anaerobic conditions.

To determine the colonization levels of the bacteria in the gut, gnotobiotic mice were checked at 1 week, 4 weeks, 8 weeks, 12 weeks, and 15 weeks after inoculation by plating appropriate serial dilutions of feces on the LB or BBE agar plates and counting the colonies after incubation. DNA extraction from feces and 16S rRNA gene PCR sequencing were performed to confirm the presence of one bacterium only in monocolonized animals (data not shown).

**Construction of the *waaG* mutant of *Enterobacter cloacae* B29.** A *waaG* deletion mutant of *Enterobacter cloacae* B29 was constructed using a positive-selection suicide vector, pKNG101 (60), which contains a *pir*-dependent R6K origin of replication (oriR6K), the *strAB* gene encoding the streptomycin phosphotransferase (Sm$^r$), an origin of transfer (mobRK2), the *sacB* gene mediating sucrose sensitivity (Suc$^s$), and multiple cloning sites. Briefly, a 619-bp DNA fragment upstream and 651-bp DNA fragment downstream of the target gene *waaG* were PCR amplified using the oligonucleotides pairs WGPA/WGPB (5′-CTAGGGCCCGATTGACCGCATT-3′/5′-GTTAGGGAAAGGATCATACGTTCGTGGCTCTGGAC-3′) and WGPC/WGPD (5′-CAATCCCTTTCCTCAATCCCTTTCCTCGAGACCTG-3′/5′-CTAGGGCCCGGAGAACATCCCGTGT-3′), respectively. The oligonucleotides WGPB and WGPC were designed for amplifying the two fragments with overlapping 3′ and 5′ ends to facilitate splicing by overlapping extension (SOE). Agarose gel-purified fragments upstream and downstream of *waaG* were ligated by performing an overlapping PCR. The resulting PCR product without the 574-bp *waaG* fragment was then cloned into the pKNG101 suicide vector. The constructs were transformed into *E. coli* SM10 λ*pir* as a donor strain via electroporation, followed by mobilization into wild-type strain B29 by conjugal mating. Integration of the suicide vector results in an Sm$^r$ and Suc$^s$ phenotype. B29/*pKNG101* recombination cells with a single chromosomal integration event were selected on agar plates containing streptomycin (50 $\mu$g ml$^{-1}$) and rifampin (100 $\mu$g ml$^{-1}$) to select against the *E. coli* SM10 λ*pir*/pKNG101 donor because of the rifampin-resistant character of B29. Sm$^r$ Suc$^s$ cells were selected and plated onto LB plates containing 10% sucrose to select cells with a second homologous recombination. Finally, Sm$^s$ Suc$^r$ cells were confirmed to contain the gene deletion by PCR and sequencing. The resulting mutant was designated the B29Δ*waaG* strain and was indistinguishable from the wild-type strain, except for the loss of a 574-bp *waaG* DNA fragment.

**LPS extraction and endotoxin activity detection.** LPS extraction from *Enterobacter cloacae* B29, the B29Δ*waaG* mutant, the *B. thetaiotaomicron* type strain (ATCC 29148), *K. pneumoniae* A7, or *Escherichia coli* PY102 was performed using the LPS extraction kit (iNtRON Biotechnology Co., Seoul, South Korea) according to the manufacturer's instructions. Endotoxin activity analyses were performed using the chromogenic substrate *Limulus* amebocyte lysate (LAL) assay (Associates of Cape Cod Incorporated, USA). The LPS derived from *E. coli* 055:B5 (L2880; phenol extract; Sigma) was used as a positive control in the assay.

**Oral glucose tolerance test and assessment of insulin secretion.** Mice were fasted for 5 h, and baseline blood glucose levels were measured with an ACCU-CHEK Performa (Roche) glucometer using blood collected from the tail vein. Glucose (2 g/kg body weight) was given orally by gavage, and blood glucose levels then were measured 15, 30, 60, 90, and 120 min after gavage. Blood was sampled before and 30 min after the glucose load to assess plasma insulin levels via enzyme-linked immunosorbent assay (ELISA).

**Serum biochemical analysis.** Serum insulin, leptin, adiponectin, and SAA-3 levels were determined by ELISA kits from Millipore Corporation (Billerica, MA). The serum LBP level was measured by a mouse lipopolysaccharide binding protein ELISA kit (HyCult Biotechnology, Uden, The Netherlands). All assays were performed according to the manufacturers' instructions.

**Liver triglyceride extraction and measurement.** Portions of frozen liver from receiver mice were homogenized in chloroform-methanol (2:1) to extract total lipids according to the methodology of Folch et al. (61). The organic extract was dried and reconstituted in isopropanol. The triglyceride content was measured with a triglyceride's determination kit (Sigma-Aldrich, Saint-Louis, MO, USA) according to the manufacturer's instructions.

**Epididymal adipose tissue histology.** Adipose tissue morphometric analysis was performed on the sections stained by hematoxylin-eosin-saffron (HES stain). Slides were digitalized using a Pannoramic digital slide scanner (3DHistech Ltd., Budapest, Hungary), and adipocyte morphometry was analyzed, quantified, and photographed using Pannoramic Viewer software by 3DHistech. The number of adipocytes per microscopic field (at least 5 fields per tissue) was determined at a magnification of ×200, and the average surface area of the adipocytes (in square micrometers) was calculated.

**TaqMan low-density array RT-qPCR assay and data analysis.** Quantitative real-time PCR (RT-qPCR) utilized a custom-made TaqMan low-density array RT-qPCR assay (TLDA) cards from Life Technologies (Thermo Fisher Scientific), by following the manufacturer's instructions, to separately examine the expression levels of 21 selected mouse genes in liver, ileum, or epididymal adipose tissue, which may be involved in metabolic syndrome development, and 3 housekeeping genes (glyceraldehyde-3-phosphate dehydrogenase [GAPDH], 18S, and ACTB) (see Table S1 in the supplemental material). In this study, the TLDA cards were configured into eight identical 24-gene sets (duplicate per sample). Briefly, each cDNA (30 $\mu$l) sample was mixed with 25 $\mu$l of $H_2O$ and 55 $\mu$l of 2× TaqMan universal PCR master mix (Applied Biosystems). Each sample (100 $\mu$l PCR mixture) then was loaded into each pool of the TLDA card. Thermal cycling was performed using an Applied Biosystems 7900HT sequence detection system for 2 min at 50°C and 10 min at 95°C, followed by 40 cycles for 15 s at 95°C and 1 min at 60°C. TLDA data were collected with the manufacturer's SDS software. RQ Manager Analysis software (Applied Biosystems) was used to process the array data and determine the threshold cycle ($C_T$) values. Thresholds, set at 0.2, were checked individually and corrected as necessary. GAPDH and 18S genes were chosen for this study, as they were identified as the least variable of all housekeeping genes included in the TLDA assays. Consequently, data were normalized against the housekeeping gene using the values of each of the 8 pools. Relative quantification of gene expression was determined using the comparative $C_T$ method, which means the fold change in gene expression in the treated group relative to the control was calculated by the equation $2^{-\Delta\Delta CT} = 2^{-[(CT \text{ target gene} - CT \text{ GAPDH})\text{treated} - (CT \text{ target gene} - CT \text{ GAPDH})\text{untreated}]}$ (62).

**Statistical analysis.** Statistical analysis was performed using SPSS statistical software package 17.0 (SPSS, Chicago, IL, USA). Normal distribution of the data was determined using the Shapiro-Wilk test. A one-way analysis of variance (ANOVA) followed by a *post hoc* (Turkey's multiple-comparison test) was used for data between multiple groups that were normally distributed, and the Kruskal-Wallis H-test was used for data that were not normally distributed. Student's *t* test (normally) or Mann-Whitney U test (not normally) was used for comparing differences between two groups. Results are expressed as means ± standard errors of the means (SEM), with statistical significance set at 0.05, 0.01, or 0.001.

The clinical study was approved by the Ethics Committee of Chinese Clinical Trial Registry (registration number ChiECRCT-000011).

## SUPPLEMENTAL MATERIAL

Supplemental material is available online only.

**FIG S1**, TIF file, 0.4 MB.

**FIG S2**, TIF file, 1.1 MB.

**FIG S3**, TIF file, 0.1 MB.

**FIG S4**, TIF file, 1.2 MB.

**FIG S5**, TIF file, 1.3 MB.

**FIG S6**, TIF file, 1 MB.

**FIG S7**, TIF file, 1.1 MB.

**FIG S8**, TIF file, 1.2 MB.

**FIG S9**, TIF file, 1.3 MB.

**TABLE S1**, DOCX file, 0.03 MB.

## ACKNOWLEDGMENTS

We are grateful to the Animal Resources Center of the University of Chicago for kindly providing the C3H/HeN TLR4$^{-/-}$ GF mice (Tatiana Golovkina, Department of Microbiology, The University of Chicago, Chicago, IL, USA, and Betty R. Theriault, Animal Resources Center, Department of Surgery, The University Of Chicago) and Anaxem, the animal facility of the Micalis Institute, for the GF male C57BL/6J mice and C3H/HeN wild-type.

This work was funded by grants from the National Natural Science Foundation of China (31300712, 31330005, 30730005, 81100632, 31121064, 20825520, and 21221064).

L.Z. directed the study, which was designed together with N.F. and P.G.; A.B., N.F., and S.R. managed and performed the mouse work; N.F. analyzed and interpreted the data; X.Z., R.W., J.W., and N.F. constructed the *waaG* mutant of *Enterobacter cloacae* B29; and N.F., P.G., and L.Z. wrote the paper.

We have no conflicts of interest to report.

## REFERENCES


1. Loomba R, Sanyal AJ. 2013. The global NAFLD epidemic. Nat Rev Gastroenterol Hepatol 10:686–690. https://doi.org/10.1038/nrgastro.2013.171.
2. Tripathi A, Debelius J, Brenner DA, Karin M, Loomba R, Schnabl B, Knight R. 2018. The gut–liver axis and the intersection with the microbiome. Nat Rev Gastroenterol Hepatol 15:397–411. https://doi.org/10.1038/s41575-018-0031-8.
3. Backhed F, Ding H, Wang T, Hooper LV, Koh GY, Nagy A, Semenkovich CF, Gordon JI. 2004. The gut microbiota as an environmental factor that regulates fat storage. Proc Natl Acad Sci U S A 101:15718–15723. https://doi.org/10.1073/pnas.0407076101.
4. Rabot S, Membrez M, Bruneau A, Gerard P, Harach T, Moser M, Raymond F, Mansourian R, Chou CJ. 2010. Germ-free C57BL/6J mice are resistant to high-fat-diet-induced insulin resistance and have altered cholesterol metabolism. FASEB J 24:4948–4959. https://doi.org/10.1096/fj.10-164921.
5. Le Roy T, Llopis M, Lepage P, Bruneau A, Rabot S, Bevilacqua C, Martin P, Philippe C, Walker F, Bado A, Perlemuter G, Cassard-Doulcier A-M, Gérard P. 2013. Intestinal microbiota determines development of non-alcoholic fatty liver disease in mice. Gut 62:1787–1794. https://doi.org/10.1136/gutjnl-2012-303816.
6. Hoyles L, Fernández-Real J-M, Federici M, Serino M, Abbott J, Charpentier J, Heymes C, Luque JL, Anthony E, Barton RH, Chilloux J, Myridakis A, Martinez-Gili L, Moreno-Navarrete JM, Benhamed F, Azalbert V, Blasco-Baque V, Puig J, Xifra G, Ricart W, Tomlinson C, Woodbridge M, Cardellini M, Davato F, Cardolini I, Porzio O, Gentileschi P, Lopez F, Foufelle F, Butcher SA, Holmes E, Nicholson JK, Postic C, Burcelin R, Dumas M-E. 2018. Molecular phenomics and metagenomics of hepatic steatosis in non-diabetic obese women. Nat Med 24:1070–1080. https://doi.org/10.1038/s41591-018-0061-3.
7. Wang R, Li H, Yang X, Xue X, Deng L, Shen J, Zhang M, Zhao L, Zhang C. 2018. Genetically obese human gut microbiota induces liver steatosis in germ-free mice fed on normal diet. Front Microbiol 9:1602. https://doi.org/10.3389/fmicb.2018.01602.
8. Chiu C-C, Ching Y-H, Li Y-P, Liu J-Y, Huang Y-T, Huang Y-W, Yang S-S, Huang W-C, Chuang H-L. 2017. Nonalcoholic fatty liver disease is exacerbated in high-fat diet-fed gnotobiotic mice by colonization with the gut microbiota from patients with nonalcoholic steatohepatitis. Nutrients 9:1220. https://doi.org/10.3390/nu9111220.
9. Safari Z, Gérard P. 2019. The links between the gut microbiome and non-alcoholic fatty liver disease (NAFLD). Cell Mol Life Sci 76:1541–1558. https://doi.org/10.1007/s00018-019-03011-w.
10. Zhu L, Baker SS, Gill C, Liu W, Alkhouri R, Baker RD, Gill SR. 2013. Characterization of gut microbiomes in nonalcoholic steatohepatitis (NASH) patients: a connection between endogenous alcohol and NASH. Hepatology 57:601–609. https://doi.org/10.1002/hep.26093.
11. Loomba R, Seguritan V, Li W, Long T, Klitgord N, Bhatt A, Dulai PS, Caussy C, Bettencourt R, Highlander SK, Jones MB, Sirlin CB, Schnabl B, Brinkac L, Schork N, Chen C-H, Brenner DA, Biggs W, Yooseph S, Venter JC, Nelson KE. 2017. Gut microbiome-based metagenomic signature for non-invasive detection of advanced fibrosis in human nonalcoholic fatty liver disease. Cell Metab 25:1054–1062. https://doi.org/10.1016/j.cmet.2017.04.001.
12. Boursier J, Mueller O, Barret M, Machado M, Fizanne L, Araujo-Perez F, Guy CD, Seed PC, Rawls JF, David LA, Hunault G, Oberti F, Calès P, Diehl AM. 2016. The severity of nonalcoholic fatty liver disease is associated with gut dysbiosis and shift in the metabolic function of the gut microbiota. Hepatology 63:764–775. https://doi.org/10.1002/hep.28356.
13. Michail S, Lin M, Frey MR, Fanter R, Paliy O, Hilbush B, Reo NV. 2015. Altered gut microbial energy and metabolism in children with non-alcoholic fatty liver disease. FEMS Microbiol Ecol 91:1–9. https://doi.org/10.1093/femsec/fiu002.
14. Zhang C, Zhao L. 2016. Strain-level dissection of the contribution of the gut microbiome to human metabolic disease. Genome Med 8:41. https://doi.org/10.1186/s13073-016-0304-1.
15. Arrese M, Cabrera D, Kalergis AM, Feldstein AE. 2016. Innate immunity and inflammation in NAFLD/NASH. Dig Dis Sci 61:1294–1303. https://doi.org/10.1007/s10620-016-4049-x.
16. Nolan JP, Leibowitz AI. 1978. Endotoxins in liver disease. Gastroenterology 75:765–766. https://doi.org/10.1016/S0016-5085(19)31709-3.
17. Pappo I, Becovier H, Berry EM, Freund HR. 1991. Polymyxin B reduces cecal flora, TNF production and hepatic steatosis during total parenteral nutrition in the rat. J Surg Res 51:106–112. https://doi.org/10.1016/0022-4804(91)90078-z.
18. Pappo I, Bercovier H, Berry EM, Haviv Y, Gallily R, Freund HR. 1992. Polymyxin B reduces total parenteral nutrition–associated hepatic steatosis by its antibacterial activity and by blocking deleterious effects of lipopolysaccharide. J Parenter Enteral Nutr 16:529–532. https://doi.org/10.1177/0148607192016006529.
19. Cani PD, Amar J, Iglesias MA, Poggi M, Knauf C, Bastelica D, Neyrinck AM, Fava F, Tuohy KM, Chabo C, Waget A, Delmee E, Cousin B, Sulpice T, Chamontin B, Ferrieres J, Tanti J-F, Gibson GR, Casteilla L, Delzenne NM, Alessi MC, Burcelin R. 2007. Metabolic endotoxemia initiates obesity and insulin resistance. Diabetes 56:1761–1772. https://doi.org/10.2337/db06-1491.
20. Kudo H, Takahara T, Yata Y, Kawai K, Zhang W, Sugiyama T. 2009. Lipopolysaccharide triggered TNF-$\alpha$-induced hepatocyte apoptosis in a murine non-alcoholic steatohepatitis model. J Hepatol 51:168–175. https://doi.org/10.1016/j.jhep.2009.02.032.
21. Abu-Shanab A, Quigley EM. 2010. The role of the gut microbiota in nonalcoholic fatty liver disease. Nat Rev Gastroenterol Hepatol 7:691–701. https://doi.org/10.1038/nrgastro.2010.172.
22. Machado MV, Cortez-Pinto H. 2012. Gut microbiota and nonalcoholic fatty liver disease. Ann Hepatol 11:440–449. https://doi.org/10.1016/S1665-2681(19)31457-7.
23. Fei N, Zhao L. 2013. An opportunistic pathogen isolated from the gut of an obese human causes obesity in germfree mice. ISME J 7:880–884. https://doi.org/10.1038/ismej.2012.153.
24. Itoh K, Mitsuoka T. 1985. Characterization of clostridia isolated from faeces of limited flora mice and their effect on caecal size when associated with germ-free mice. Lab Anim 19:111–118. https://doi.org/10.1258/002367785780942589.
25. Mencin A, Kluwe J, Schwabe RF. 2009. Toll-like receptors as targets in chronic liver diseases. Gut 58:704–720. https://doi.org/10.1136/gut.2008.156307.
26. Kong Q, Yang J, Liu Q, Alamuri P, Roland KL, Curtiss R. 2011. Effect of deletion of genes involved in lipopolysaccharide core and O-antigen synthesis on virulence and immunogenicity of Salmonella enterica serovar Typhimurium. Infect Immun 79:4227–4239. https://doi.org/10.1128/IAI.05398-11.
27. Liebau J, Fu B, Brown C, Mäler L. 2018. New insights into the membrane association mechanism of the glycosyltransferase WaaG from Escherichia coli. Biochim Biophys Acta Biomembr 1860:683–690. https://doi.org/10.1016/j.bbamem.2017.12.004.
28. Rivera CA, Adegboyega P, van Rooijen N, Tagalicud A, Allman M, Wallace M. 2007. Toll-like receptor-4 signaling and Kupffer cells play pivotal roles in the pathogenesis of non-alcoholic steatohepatitis. J Hepatol 47:571–579. https://doi.org/10.1016/j.jhep.2007.04.019.
29. Shi H, Kokoeva MV, Inouye K, Tzameli I, Yin H, Flier JS. 2006. TLR4 links innate immunity and fatty acid–induced insulin resistance. J Clin Investig 116:3015–3025. https://doi.org/10.1172/JCI28898.
30. Suganami T, Tanimoto-Koyama K, Nishida J, Itoh M, Yuan X, Mizuarai S, Kotani H, Yamaoka S, Miyake K, Aoe S, Kamei Y, Ogawa Y. 2007. Role of the Toll-like receptor 4/NF-$\kappa$B pathway in saturated fatty acid-induced inflammatory changes in the interaction between adipocytes and macrophages. Arterioscler Thromb Vasc Biol 27:84–91. https://doi.org/10.1161/01.ATV.0000251608.09329.9a.
31. Cani PD, Bibiloni R, Knauf C, Waget A, Neyrinck AM, Delzenne NM, Burcelin R. 2008. Changes in gut microbiota control metabolic endotoxemia-induced inflammation in high-fat diet-induced obesity and diabetes in mice. Diabetes 57:1470–1481. https://doi.org/10.2337/db07-1403.
32. Kim F, Pham M, Luttrell I, Bannerman DD, Tupper J, Thaler J, Hawn TR, Raines EW, Schwartz MW. 2007. Toll-like receptor-4 mediates vascular inflammation and insulin resistance in diet-induced obesity. Circ Res 100:1589–1596. https://doi.org/10.1161/CIRCRESAHA.106.142851.
33. Blechova R, Pivodova D. 2001. Limulus amoebocyte lysate (LAL) test–an alternative method for detection of bacterial endotoxins. Acta Veterinaria Brno 70:291–296. https://doi.org/10.2754/avb200170030291.
34. Schumann RR, Leong SR, Flaggs GW, Gray PW, Wright SD, Mathison JC, Tobias PS, Ulevitch RJ. 1990. Structure and function of lipopolysaccha-

ride binding protein. Science 249:1429–1431. https://doi.org/10.1126/science.2402637.
35. Vatanen T, DIABIMMUNE Study Group, Kostic AD, d'Hennezel E, Siljander H, Franzosa EA, Yassour M, Kolde R, Vlamakis H, Arthur TD, Hämäläinen A-M, Peet A, Tillmann V, Uibo R, Mokurov S, Dorshakova N, Ilonen J, Virtanen SM, Szabo SJ, Porter JA, Lähdesmäki H, Huttenhower C, Gevers D, Cullen TW, Knip M, Xavier RJ. 2016. Variation in microbiome LPS immunogenicity contributes to autoimmunity in humans. Cell 165:842–853. https://doi.org/10.1016/j.cell.2016.04.007.
36. Lindberg AA, Weintraub A, Zahringer U, Rietschel ET. 1990. Structure-activity relationships in lipopolysaccharides of Bacteroides fragilis. Rev Infect Dis 12(Suppl 2):S133–S141. https://doi.org/10.1093/clinids/12.supplement_2.s133.
37. Samuel BS, Gordon JI. 2006. A humanized gnotobiotic mouse model of host-archaeal-bacterial mutualism. Proc Natl Acad Sci U S A 103:10011–10016. https://doi.org/10.1073/pnas.0602187103.
38. Kolodziejczyk AA, Zheng D, Shibolet O, Elinav E, Kolodziejczyk AA, Zheng D, Shibolet O, Elinav E. 2019. The role of the microbiome in NAFLD and NASH. EMBO Mol Med 11:e9302. https://doi.org/10.15252/emmm.201809302.
39. Sanders WE, Sanders CC. 1997. Enterobacter spp.: pathogens poised to flourish at the turn of the century. Clin Microbiol Rev 10:220–241. https://doi.org/10.1128/CMR.10.2.220.
40. Liu R, Hong J, Xu X, Feng Q, Zhang D, Gu Y, Shi J, Zhao S, Liu W, Wang X, Xia H, Liu Z, Cui B, Liang P, Xi L, Jin J, Ying X, Wang X, Zhao X, Li W, Jia H, Lan Z, Li F, Wang R, Sun Y, Yang M, Shen Y, Jie Z, Li J, Chen X, Zhong H, Xie H, Zhang Y, Gu W, Deng X, Shen B, Xu X, Yang H, Xu G, Bi Y, Lai S, Wang J, Qi L, Madsen L, Wang J, Ning G, Kristiansen K, Wang W. 2017. Gut microbiome and serum metabolome alterations in obesity and after weight-loss intervention. Nat Med 23:859–868. https://doi.org/10.1038/nm.4358.
41. Evans AS. 1976. Causation and disease: the Henle-Koch postulates revisited. Yale J Biol Med 49:175–195.
42. Vonaesch P, Anderson M, Sansonetti PJ. 2018. Pathogens, microbiome and the host: emergence of the ecological Koch's postulates. FEMS Microbiol Rev 42:273–292. https://doi.org/10.1093/femsre/fuy003.
43. Seki E, De Minicis S, Österreicher CH, Kluwe J, Osawa Y, Brenner DA, Schwabe RF. 2007. TLR4 enhances TGF-$\beta$ signaling and hepatic fibrosis. Nat Med 13:1324–1332. https://doi.org/10.1038/nm1663.
44. Isayama F, Hines IN, Kremer M, Milton RJ, Byrd CL, Perry AW, McKim SE, Parsons C, Rippe RA, Wheeler MD. 2006. LPS signaling enhances hepatic fibrogenesis caused by experimental cholestasis in mice. Am J Physiol Gastrointest Liver Physiol 290:G1318–G1328. https://doi.org/10.1152/ajpgi.00405.2005.
45. Zhai Y, Shen X-D, O'Connell R, Gao F, Lassman C, Busuttil RW, Cheng G, Kupiec-Weglinski JW. 2004. Cutting edge: TLR4 activation mediates liver ischemia/reperfusion inflammatory response via IFN regulatory factor 3-dependent MyD88-independent pathway. J Immunol 173:7115–7119. https://doi.org/10.4049/jimmunol.173.12.7115.
46. Spruss A, Kanuri G, Wagnerberger S, Haub S, Bischoff SC, Bergheim I. 2009. Toll-like receptor 4 is involved in the development of fructose-induced hepatic steatosis in mice. Hepatology 50:1094–1104. https://doi.org/10.1002/hep.23122.
47. Raffatellu M, Santos RL, Verhoeven DE, George MD, Wilson RP, Winter SE, Godinez I, Sankaran S, Paixao TA, Gordon MA, Kolls JK, Dandekar S, Bäumler AJ. 2008. Simian immunodeficiency virus-induced mucosal interleukin-17 deficiency promotes Salmonella dissemination from the gut. Nat Med 14:421–428. https://doi.org/10.1038/nm1743.
48. Chi W, Dao D, Lau TC, Henriksbo BD, Cavallari JF, Foley KP, Schertzer JD. 2014. Bacterial peptidoglycan stimulates adipocyte lipolysis via NOD1. PLoS One 9:e97675. https://doi.org/10.1371/journal.pone.0097675.
49. Chen Y-M, Liu Y, Zhou R-F, Chen X-L, Wang C, Tan X-Y, Wang L-J, Zheng R-D, Zhang H-W, Ling W-H, Zhu H-L. 2016. Associations of gut-flora-dependent metabolite trimethylamine-N-oxide, betaine and choline with non-alcoholic fatty liver disease in adults. Sci Rep 6:19076. https://doi.org/10.1038/srep19076.
50. Wahlström A, Sayin SI, Marschall H-U, Bäckhed F. 2016. Intestinal crosstalk between bile acids and microbiota and its impact on host metabolism. Cell Metab 24:41–50. https://doi.org/10.1016/j.cmet.2016.05.005.
51. Sahuri-Arisoylu M, Brody L, Parkinson J, Parkes H, Navaratnam N, Miller AD, Thomas E, Frost G, Bell J. 2016. Reprogramming of hepatic fat accumulation and "browning" of adipose tissue by the short-chain fatty acid acetate. Int J Obes 40:955–963. https://doi.org/10.1038/ijo.2016.23.
52. Lake AD, Novak P, Shipkova P, Aranibar N, Robertson DG, Reily MD, Lehman-McKeeman LD, Vaillancourt RR, Cherrington NJ. 2015. Branched chain amino acid metabolism profiles in progressive human nonalcoholic fatty liver disease. Amino Acids 47:603–615. https://doi.org/10.1007/s00726-014-1894-9.
53. Volynets V, Küper MA, Strahl S, Maier IB, Spruss A, Wagnerberger S, Königsrainer A, Bischoff SC, Bergheim I. 2012. Nutrition, intestinal permeability, and blood ethanol levels are altered in patients with nonalcoholic fatty liver disease (NAFLD). Dig Dis Sci 57:1932–1941. https://doi.org/10.1007/s10620-012-2112-9.
54. Miele L, Valenza V, La Torre G, Montalto M, Cammarota G, Ricci R, Mascianà R, Forgione A, Gabrieli ML, Perotti G, Vecchio FM, Rapaccini G, Gasbarrini G, Day CP, Grieco A. 2009. Increased intestinal permeability and tight junction alterations in nonalcoholic fatty liver disease. Hepatology 49:1877–1887. https://doi.org/10.1002/hep.22848.
55. Luther J, Garber JJ, Khalili H, Dave M, Bale SS, Jindal R, Motola DL, Luther S, Bohr S, Jeoung SW, Deshpande V, Singh G, Turner JR, Yarmush ML, Chung RT, Patel SJ. 2015. Hepatic injury in nonalcoholic steatohepatitis contributes to altered intestinal permeability. Cell Mol Gastroenterol Hepatol 1:222–232. https://doi.org/10.1016/j.jcmgh.2015.01.001.
56. Parker R. 2018. The role of adipose tissue in fatty liver diseases. Liver Res 2:35–42. https://doi.org/10.1016/j.livres.2018.02.002.
57. Donnelly KL, Smith CI, Schwarzenberg SJ, Jessurun J, Boldt MD, Parks EJ. 2005. Sources of fatty acids stored in liver and secreted via lipoproteins in patients with nonalcoholic fatty liver disease. J Clin Investig 115:1343–1351. https://doi.org/10.1172/JCI23621.
58. Boden G, She P, Mozzoli M, Cheung P, Gumireddy K, Reddy P, Xiang X, Luo Z, Ruderman N. 2005. Free fatty acids produce insulin resistance and activate the proinflammatory nuclear factor-κB pathway in rat liver. Diabetes 54:3458–3465. https://doi.org/10.2337/diabetes.54.12.3458.
59. Kawano Y, Cohen DE. 2013. Mechanisms of hepatic triglyceride accumulation in non-alcoholic fatty liver disease. J Gastroenterol 48:434–441. https://doi.org/10.1007/s00535-013-0758-5.
60. Kaniga K, Delor I, Cornelis GR. 1991. A wide-host-range suicide vector for improving reverse genetics in gram-negative bacteria: inactivation of the blaA gene of Yersinia enterocolitica. Gene 109:137–141. https://doi.org/10.1016/0378-1119(91)90599-7.
61. Folch J, Lees M, Sloane Stanley G. 1957. A simple method for the isolation and purification of total lipides from animal tissues. J Biol Chem 226:497–509.
62. Schmittgen TD, Livak KJ. 2008. Analyzing real-time PCR data by the comparative CT method. Nat Protoc 3:1101–1108. https://doi.org/10.1038/nprot.2008.73.